Video Article

Switchable Acoustic and Optical Resolution Photoacoustic Microscopy for *In Vivo* Small-animal Blood Vasculature Imaging

Mohesh Moothanchery[1], Arunima Sharma[1], Manojit Pramanik[1]

[1]School of Chemical and Biomedical Engineering, Nanyang Technological University

Correspondence to: Manojit Pramanik at manojit@ntu.edu.sg

URL: https://www.jove.com/video/55810
DOI: doi:10.3791/55810

Keywords: Bioengineering, Issue 124, Acoustic resolution photoacoustic microscopy, optical resolution photoacoustic microscopy, photoacoustic imaging, photoacoustics, *in vivo* imaging, AR-PAM, OR-PAM, microscopy, combined microscopy system

Date Published: 6/26/2017

Citation: Moothanchery, M., Sharma, A., Pramanik, M. Switchable Acoustic and Optical Resolution Photoacoustic Microscopy for *In Vivo* Small-animal Blood Vasculature Imaging. *J. Vis. Exp.* (124), e55810, doi:10.3791/55810 (2017).

Abstract

Photoacoustic microscopy (PAM) is a fast-growing *invivo* imaging modality that combines both optics and ultrasound, providing penetration beyond the optical mean free path (~1 mm in skin) with high resolution. By combining optical absorption contrast with the high spatial resolution of ultrasound in a single modality, this technique can penetrate deep tissues. Photoacoustic microscopy systems can have either a low acoustic resolution and probe deeply or a high optical resolution and probe shallowly. It is challenging to achieve high spatial resolution and large depth penetration with a single system. This work presents an AR-OR-PAM system capable of both high-resolution imaging at shallow depths and low-resolution deep-tissue imaging of the same sample *in vivo*. A lateral resolution of 4 µm with 1.4 mm imaging depth using optical focusing and a lateral resolution of 45 µm with 7.8 mm imaging depth using acoustic focusing were successfully demonstrated using the combined system. Here, *in vivo* small-animal blood vasculature imaging is performed to demonstrate its biological imaging capability.

Video Link

The video component of this article can be found at https://www.jove.com/video/55810/

Introduction

High-resolution optical imaging modalities, such as optical coherence tomography, confocal microscopy, and multiphoton microscopy, have numerous benefits. However, the spatial resolution decreases significantly as the imaging depth increases. This is because of the diffuse nature of light transport in soft tissues[1,2]. The integration of optical excitation and ultrasound detection provides a solution to overcome the challenge of high-resolution optical imaging in deep tissues. Photoacoustic microscopy (PAM) is one such modality that can provide deeper imaging than other optical imaging modalities. It has been successfully applied to *in vivo* structural, functional, molecular, and cell imaging[3,4,5,6,7,8,9,10,11,12,13] studies by combining the strong optical absorption contrast with the high spatial resolution from ultrasound.

In PAM, a short laser pulse irradiates the tissue/sample. The absorption of light by chromophores (*e.g.,* melanin, hemoglobin, water *etc.*) results in a temperature increase, which in turn results in the production of pressure waves in the form of acoustics waves (photoacoustic waves). The generated photoacoustic waves can be detected by a wideband ultrasonic transducer outside the tissue boundary. Utilizing weak optical and tight acoustic focusing, deep-tissue imaging can be achieved in acoustic resolution photoacoustic microscopy (AR-PAM)[14,15,16]. In AR-PAM, a lateral resolution of 45 µm and an imaging depth up to 3 mm have been demonstrated[15]. In order to resolve single capillaries (~5 µm) acoustically, ultrasonic transducers operating at >400 MHz central frequencies are required. At such high frequencies, the penetration depth is less than 100 µm. The problem caused by tight acoustic focusing can be resolved using tight optical focusing. Optical resolution photoacoustic microscopy (OR-PAM) is capable of resolving single capillaries, or even a single cell[17], and a lateral resolution of 0.5 µm has been achieved[18,19,20,21,22,23,24]. The use of a photonic nanojet can help to achieve a resolution beyond the diffraction-limited resolution[25,26]. In OR-PAM, the penetration depth is limited due to light focusing, and it can image up to ~1.2 mm inside the biological tissue[23]. Therefore, AR-PAM can image deeper, but with a lower resolution, and OR-PAM can image with a very high resolution, but with limited imaging depth. The imaging speed of the AR and OR-PAM system mainly depends upon the pulse repetition rate of the laser source[27].

Combining AR-PAM and OR-PAM will be of great benefit to applications that require both a high resolution and deeper imaging. Little effort has been made to combine these systems together. Usually, two different imaging scanners are used for imaging, which requires that the sample be moved between both systems, thus making it difficult to perform *in vivo* imaging. However, hybrid imaging with both AR and OR PAM enables imaging with scalable resolutions and depths. In one approach, an optical fiber bundle is used to deliver light for both the AR and OR PAM. In this approach, two separate lasers (a high-energy laser at 570 nm for the AR and a low-energy, high-repetition rate laser at 532 nm for the OR) are used, making the system inconvenient and expensive[28]. The OR-PAM laser wavelength is fixed, and many studies, such as on oxygen saturation, are not possible using this combined system. Comparative studies between AR and OR PAM are also not possible because of the difference in laser wavelengths between the AR and OR. Moreover, AR-PAM uses bright-field illumination; hence, strong photoacoustic signals from the skin surface limit the image quality. For this reason, the system cannot be used for many bioimaging applications. In another approach to perform AR and OR PAM, the optical and ultrasound focus is shifted, which makes the light focus and ultrasound focus unaligned. Thus, the

image quality is not optimal[29]. Using this technique, the AR-PAM and OR-PAM can achieve only 139 µm and 21-µm resolutions, respectively, making it a poor-resolution system. Another approach, which includes changing the optical fiber and collimating optics, was reported to switch between AR and OR PAM, making the alignment process difficult[30]. In all of these cases, AR-PAM did not use dark-field illumination. The use of dark-field illumination can reduce the generation of strong photoacoustic signals from the skin surface. Therefore, deep-tissue imaging can be performed using ring-shaped illumination, as the detection sensitivity of deep photoacoustic signals will be higher compare to that of bright-field illumination.

This work reports a switchable AR and OR PAM (AR-OR-PAM) imaging system capable of both high-resolution imaging and low-resolution deep-tissue imaging of the same sample, using the same laser and scanner for both systems. The performance of the AR-OR-PAM system was characterized by determining the spatial resolution and imaging depth using phantom experiments. *In vivo* blood vasculature imaging was performed on a mouse ear to demonstrate its biological imaging capability.

Protocol

All animal experiments were performed according to the approved regulations and guidelines of the Institutional Animal Care and Use Committee of Nanyang Technological University, Singapore (Animal Protocol Number ARF-SBS/NIE-A0263).

1. AR-OR-PAM System (Figure 1)

1. **System configuration: AR-PAM**
    1. Use a nanosecond tunable laser system consisting of a diode-pumped, solid-state Nd-YAG laser (532 nm) and a dye laser with a tunability range of 559-576 nm as the optical irradiation source. Set the laser wavelength to 570 nm using an external controller and the repetition rate of the laser to 1 kHz using the laser software.
    2. Place a beam sampler at a 45° angle in front of the laser to divert 5% of the laser power to a photodiode through a variable neutral density filter (NDF1; OD = 0-4.0).
    3. Divert the laser beam after the beam sampler at 90° using a right-angle prism (RAP1).
    4. Use another right-angle prism (RAP2) to allow the beam to pass through a variable neutral density filter (NDF2; OD = 0-4.0) and onto a multimode fiber (MMF), directing it through a fiber coupler (FC)-a combination of objectives (numerical aperture (NA): 0.25) and an XY translator.
    5. Fix the fiber onto the scanning stage using an XY translator. Place a plano-convex lens (L1) 25 mm away from the fiber output end to collimate the beam out of the fiber.
    6. Pass the collimated beam through a conical lens with an apex angle of 130° to generate a ring-shaped beam. Weakly focus the ring-shaped beam onto the subject using a homemade optical condenser (OC) with cone angles of 70° and 110° and with a hole in the center.
    7. Place a 50 MHz ultrasonic transducer (UST) with an acoustic lens (AL) at the center of the homemade condenser.

2. **System configuration: OR-PAM**
    1. Use a nanosecond tunable laser system consisting of a diode-pumped, solid-state Nd-YAG laser (532 nm) and a dye laser with a tunability range of 559 - 576 nm as the optical irradiation source. Set the laser wavelength at 570 nm using an external controller and the repetition rate of the laser at 5 kHz using the laser software.
    2. Rotate the computer-controlled rotational stage (holding the RAP1) by 90° to divert the laser beam onto an iris for reshaping.
    3. Attenuate the laser beam placing a variable neutral density filter (OD: 0-4.0) along the beam and then focus the beam with a condenser lens (CL). Pass it through a pinhole (PH) 75 mm away from the CL for spatial filtering.
    4. Launch the spatially filtered beam onto a single-mode fiber (SMF) using a single-mode fiber coupler (FC) consisting of a 0.1 NA objective to focus the light beam on to the SMF.
    5. Adjust the fiber coupler to achieve maximum coupling efficiency.
    6. Fix the fiber out onto the scanning stage using a slip plate (SP). Place an achromatic lens (L2) 50 mm away from the SM fiber to collimate the laser beam.
    7. Divert the collimated beam by 90° using a kinematic controllable elliptical mirror (M) to fill the back aperture of another identical achromatic lens (L3). Place the achromatic lens used for focusing on a translation mount (TM2) using a lens tube (LT).
    8. Pass the focusing beam through a homemade optoacoustic beam combiner consisting of a right-angled prism (RA) and a rhomboid prism (RP), with a layer of silicon oil (SO) in between.
    NOTE: The silicon oil layer will act as optically transparent and acoustically reflective film.
    9. Attach an acoustic lens (AL) to provide acoustic focusing (focal diameter: ~46 µm) at the bottom of the rhomboid prism.
    10. Place the ultrasonic transducer with a 50 MHz center frequency on top of the rhomboid prism; use an epoxy layer for effective coupling.

2. System Switching and Alignment

1. Fix (by screwing tightly) the homemade switchable plate to a 3-axis motorized stage controlled by a 3-axis controller connected to the computer.
2. Attach the AR and OR cage system to the homemade plate using cage mounting brackets to allow for easy switching between the AR and OR scan heads. Slide the scan head on top of the imaging area.
3. Use the Z-stage to submerge the bottom part of the AR-OR-PAM scanner head in a water-filled acrylic tank (13 cm x 30 cm x 3 cm) for acoustic coupling.
4. Open an imaging window with a 7-cm diameter on the bottom plate of the tank and seal it with a polyethylene membrane for optical and acoustic transmission.
5. **Use a pulse-echo amplifier and an oscilloscope to align the ultrasound transducer in focus.**

1. Set the gain in pulse echo amplifier to 24 db in the transmission/receiving mode.
2. Use the sync-out signal from the pulse-echo amplifier as the trigger and detect the backscattered signal from a glass slide (inserted from the bottom of water tank) using an oscilloscope.
   NOTE: The slide should have black tape stuck to it.
3. Move the Z-axis to maximize the amplitude of the pulse-echo signal (viewed on the oscilloscope).
   NOTE: When the glass plate is in focus, the echo will have its maximum amplitude.

6. Switch on the laser and connect the UST to two amplifiers, each with 24 dB fixed gain, using BNC cables.
   NOTE: The outputs of the amplifiers are connected to the data acquisition card (DAQ).
7. Use the signal from the photodiode (PD) placed in front of the laser as a trigger for the data acquisition system.
8. **In AR-PAM, vary the distance between the conical lens (con.L) and the optical condenser (OC) to maximize the amplitude of the photoacoustic signal generated from the test object (black tape stuck on a glass slide). Ensure that the optical and acoustic focuses are confocal by determining the maximum photoacoustic (PA) signal amplitude.**
   1. Note the delay of the maximum PA signals; use this later to check the focus in the data acquisition software.

9. Loosen the screw of scanning head and manually switch the scanning head from AR-PAM to OR-PAM. Then, tighten the screws.
10. **In OR-PAM, vary the distance between the focusing achromatic doublet (inside the lens tube (LT)) and the optoacoustic combiner to maximize the PA signal amplitude shown on the oscilloscope.**
    1. Note the delay of the maximum PA signals.
       NOTE: Finetuning is necessary to determine the confocal arrangement.

3. Experimental Steps

1. **Lateral resolution and imaging depth quantification**
   1. Use gold nanoparticles 100 nm in diameter to determine the lateral resolution of the AR and OR system.
   2. Dilute 0.1 mL of nanoparticle solution with an equal amount of water. Distribute 0.1 mL of diluted solution on a cover slip and place it in contact with the polyethylene membrane under the tank.
   3. Make sure that the AR-PAM and OR-PAM is in focus in the data acquisition software (see the Table of Materials) before scanning (steps 2.8 and 2.10).
      NOTE: By knowing the microsecond delay of the maximum PA signals from steps 2.9 and 2.10, multiplied by the sampling rate (250 MS/s), the image will be in focus in the data acquisition software. The delay which that must be omitted during data acquisition can be determined in the software so as to save only the necessary data points for post-processing.
   4. Set the scan parameters for the AR-PAM and press the "scan" button to start raster scanning.
      1. Set the scan parameters for the AR-PAM in the data acquisition software at "4" mm/s scanning speed in the "velocity" tab, "1" kHz in the "pulse repetition rate" tab, "0.5" mm in the "Y-scan range" tab, and "0.5" mm in the "X-scan range" tab. Set the step size in the x-direction at "4" µm in the "dx" tab.
         NOTE: The step size in the y-direction is automatically determined from the scan speed velocity of the stage and the pulse repetition rate (in this case, 4,000 µm/1,000 Hz = 4 µm)

   5. Set the scan parameters for the OR-PAM and press the "scan" button to start raster scanning.
      1. Set the scan parameters in the data acquisition software at "2.5" mm/s scanning speed in the "velocity" tab, "5" kHz in the "pulse repetition rate" tab, "0.5" mm in the "Y-scan range" tab, and "0.5" mm in the "X-scan range" tab. Set the step size in the x-direction a "0.5" µm in the "dx" tab.
         NOTE: The step size in the y-direction is automatically determined from the scan speed velocity of the stage and the pulse repetition rate (in this case, 2,500 µm/5,000 Hz = 0.5 µm).

   6. Ensure that during the scanning process, the data is continuously captured and stored on the computer
      NOTE: Data will be captured only in one direction of motion of the Y-stage.
   7. Use the multiple B-scan data stored in the computer to retrieve the maximum amplitude projection (MAP) images using image processing software (see the **Table of Materials**).
   8. Use a single nanoparticle image (out of multiple images) from the scan to determine the lateral resolution by manually plotting a line through the central region of the nanoparticle image to obtain a point-spread function, which looks like Gaussian curve. See **Figure 2**.
   9. Fit the point-spread function obtained from a single nanoparticle image using a Gaussian fit function and measure the full width at half maximum (FWHM) using image processing software (see the **Table of Materials**). Use this as the lateral resolution. See **Figure 2**.
   10. Insert a piece of black tape obliquely onto a piece of sliced chicken tissue as the target object for depth imaging. Place the tissue with the tape in the water tank.
       NOTE: The black tape is stuck to a metal plate with a sharp tip, which helps to attach the tape to the tissue.
   11. Set the scan parameters for the AR-PAM into the data acquisition software and then press the "scan" button to capture a single B-scan image to determine the maximum imaging depth.
       1. Set the scan parameters at "15" mm/s scanning speed in the "velocity" tab, "1" kHz in the "pulse repetition rate" tab, "5" cm in the "Y-scan range" tab, and "0.1" mm in the "X-scan range" tab. Set the step size in the x-direction at "0.1" mm in the "dx" tab.

   12. Set the scan parameters for the OR-PAM and press the "scan" button to capture a single B-scan image to determine the maximum imaging dept.
       1. Set the scan parameters in the data acquisition software as "15" mm/s scanning speed in the "velocity" tab, "5" kHz in the "pulse repetition rate" tab, "2" cm in the "Y-scan range" tab and "0.1" mm in the "X-scan range" tab. Set the step size in the x-direction at "0.1" mm in the "dx" tab.

NOTE: Since the X-scan range and dx are the same, only one B-scan will be captured. The time-resolved PA signals multiplied by the speed of sound in soft tissue (1,540 m/s) will give an A-line image. Multiple A-lines are captured during the continuous motion of the Y-stage to produce a B-scan.

2. ***In vivo* imaging of the mouse ear blood vasculature**
    1. Use a female mouse with a bodyweight of 25 g and an age of 4 weeks.
    2. Anesthetize the animal using a cocktail of ketamine (120 mg/kg) and xylazine (16 mg/kg) injected intraperitoneally (dosage of 0.1 mL/10 g).
    3. Remove the hair from the animal ear using hair removal cream. Wipe the area clean. Cover the eye of the animal with a sterile ocular ointment to avoid any scattered laser beam falling onto the eyes.
    4. Position the animal on a stage that also has a miniature plate to position the ear.
    5. Maintain anesthesia with inhaled isoflurane (0.75% in 1 L/min oxygen) during the imaging period.
    6. Clamp a pulse oximeter to the mouse leg or tail and monitor the physiological status. Allow the imaging region to be in contact with the polyethylene membrane using ultrasound gel.
    7. Set the scan parameters for the AR-PAM and press the "scan" button to start raster scanning.
        1. Set the scan parameters for the AR-PAM in the data acquisition software at "15" mm/s scanning speed in the "velocity" tab, "1" kHz in the "pulse repetition rate" tab, "10 mm" in the "Y-scan range" tab, and "6" mm in the "X-scan range" tab. Set the step size in the x-direction as "30" µm in the "dx" tab.
        NOTE: The step size in the y-direction is automatically determined from the scan speed velocity of the stage and the pulse repetition rate (in this case, 15,000 µm/1,000 Hz = 15 µm).
    8. After finishing AR-PAM scan, switch the imaging head position from AR-PAM to OR-PAM (as described in section 2).
    9. Set the scan parameters for the OR-PAM and press the "scan" button to start raster scanning.
        1. Set the scan parameters for the OR-PAM in the data acquisition software at "15" mm/s scan speed in the "velocity" tab, "5" kHz in the "pulse repetition rate" tab, "10" mm in the "Y-scan range" tab, and "6" mm in the "X-scan range" tab. Set the step size in the x-direction as "6" µm in the "dx" tab.
        NOTE: The step size in the y-direction is automatically determined from the scan speed velocity of the stage and the pulse repetition rate (in this case, 15,000 µm/5,000 Hz = 2 µm).
    10. Use the multiple B-scan data stored in the computer to retrieve the MAP images using image processing software.
    11. Observe the animal during the entire imaging period.

Representative Results

The schematic of the AR-OR-PAM system is shown in **Figure 1**. In this setup, all components were integrated and assembled in an optical cage setup. The use of a cage system makes the AR-OR-PAM scanning head compact and easily assembled, aligned, and integrated onto a single scanning stage.

Two-dimensional continuous raster scanning of the imaging head was used during image acquisition. The time-resolved PA signals were multiplied by the speed of sound (1,540 m/s) to obtain an A-line. Multiple A-lines captured during the continuous motion of the Y-stage produced the two-dimensional B-scan. Multiple B-scans of the imaging area were captured and stored in the computer and were used to process and produce the MAP photoacoustic images.

To determine the resolution of the switchable system, the MAP image of a single nanoparticle was used[31]. The photoacoustic amplitude along the central lateral direction of the image was plotted and fitted to a Gaussian function. The FWHM of the Gaussian fit was considered the lateral resolution. The measured lateral resolution for the AR-PAM was 45 µm, as shown in **Figure 2a**. Similarly, a single nanoparticle image acquired using OR-PAM was fitted along the central lateral direction to determine the resolution of the OR-PAM, as shown in **Figure 2b**. The measured lateral resolution was 4 µm, determined from the FWHM. The inset of the figure shows the corresponding MAP image of the gold nanoparticle. Theoretically, the optical diffraction-limited lateral resolution for AR-PAM is 45 µm, determined using the following equation: $0.72\lambda/NA$, where λ is the central acoustic wavelength and NA is the numerical aperture of the ultrasonic transducer. The theoretical resolution agrees well with the experimental data. Similarly, the theoretical lateral resolution for OR-PAM is 2.6 µm, as calculated with the following equation: $0.51\lambda/NA$, where λ is the laser wavelength and NA is the numerical aperture of the objective. The experimentally measured lateral resolution for OR-PAM was poorer than the diffraction-limit estimate, which might be due to wavefront aberrations. Since both AR and OR use a similar transducer and acoustic lens, the theoretical axial resolution will be 30 µm according to $0.88c/\Delta f$, where c is the speed of sound in soft tissue and Δf is the frequency bandwidth of the ultrasonic transducer. Additionally, the lateral resolution will vary along the axial direction for both OR-PAM[20] and AR-PAM[32]. The reported lateral resolutions here are on the focal plane.

To determine the imaging depth of the AR-OR PAM system, black tape was placed obliquely onto chicken tissue. **Figure 3a** shows the photograph of the black tape on chicken tissue. A single B-scan image was captured using both AR-PAM and OR-PAM. **Figure 3b** and **Figure 3c** shows the single B-scan PA image of AR-PAM and OR-PAM, respectively. It is evident from **Figure 3b** that the AR-PAM system can clearly image the black tape down to ~7.8 mm beneath the tissue surface. Similarly, using the OR-PAM system, it was possible to clearly image the black tape down to ~ 1.4 mm beneath the tissue surface (**Figure 3c**). The signal-to-noise ratio (SNR) was also determined from the images. SNR is defined as *V/n*, where *V* is the peak-to-peak PA signal amplitude and *n* is the standard deviation of the background noise.The SNR measured at 4.6 mm and 7.8 mm imaging depths were 2.6 and 1.4, respectively. For OR-PAM, the SNR at a 1.4-mm imaging depth was 1.4. To demonstrate the biological imaging capability of the switchable AR-OR PAM system, *in vivo* blood vasculature imaging was performed on a mouse ear. A photograph showing the vascular anatomy of the living mouse ear used for imaging is shown in **Figure 4a**. Using AR-PAM, a 10 mm x 6 mm scan region was imaged, with a step size of 15 µm in the Y-direction and 30 µm in the X-direction. The imaging took 10 min to complete. Currently, the imaging system acquires data only in one direction; the acquisition time can be reduced to almost half by modifying the program to have a bi-directional data acquisition capability. A MAP image of AR-PAM is show in **Figure 4b**. The close-up of the region of interest is shown in **Figure 4c**. A similar area scanned using OR-PAM, with a step size of 3 µm in the Y-direction and 6 µm in the X-direction, is shown in **Figure 4d**. The imaging took 46 min to complete. The close-up of the region of interest is shown in **Figure 4e**. OR-PAM can clearly resolve single capillaries, which AR-PAM cannot resolve. AR-PAM can resolve vessels thicker than 45 µm.

In summary, a switchable AR-OR-PAM system that can achieve high-resolution imaging utilizing tight optical focusing, as well as deep-tissue imaging using acoustic focusing, has been developed. The performance of the switchable AR-OR-PAM system was quantified using lateral resolution and imaging depth measurements. *In vivo* studies were also performed to show its biological imaging capability. This switchable photoacoustic microscopy system can provide high temporal and spatial resolution, making the system important for applications including the imaging of angiogenesis, drug response, *etc.*, where imaging single capillaries as well as deep vasculatures is important. Further modifications or improvement to the system can be done by replacing the homemade switchable plate with a 10 cm travelling motorized stage (y-axis). The lateral resolution of the OR-PAM can be further improved by correcting the wavefront aberrations. Delivering a higher pulse energy to the AR-PAM will improve the SNR and imaging depths as well.

In the case of OR-PAM, assuming the optical focus is 150 µm below the skin surface for *in vivo* imaging, the surface spot size was 22.5 µm in diameter. Delivering a single laser pulse of 90 nJ gives a maximum pulse energy of 20.4 mJ/cm^2. For AR-PAM, the laser focus was 2 mm in diameter. Delivering a single laser pulse of 50 µJ gives a maximum pulse energy at the focal point of 1.6 mJ/cm^2, well within the ANSI safety limit of 20 mJ/cm^2.[33].

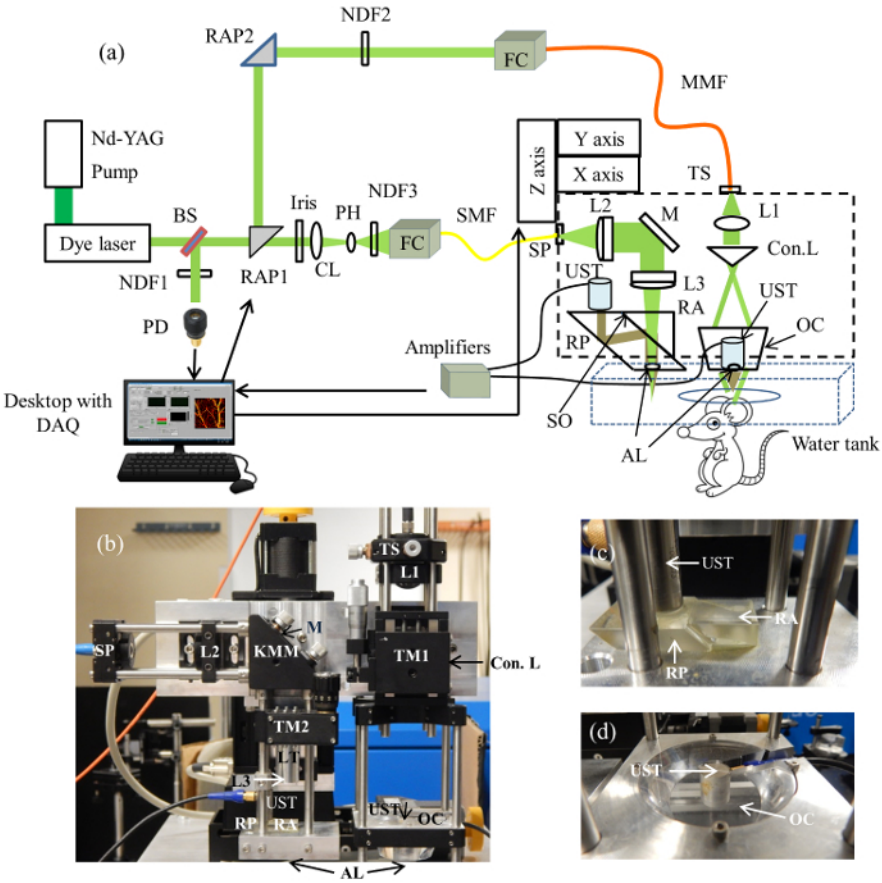

Figure 1: Schematic of the AR-OR-PAM Imaging System. (**a**) BS: beam sampler, NDF: neutral density filter, RAP - Right angle prism, PD: photodiode, CL: condenser lens, PH: pinhole, FC: fiber coupler, UST: ultrasound transducer, MMF: multimode fiber, SMF: single-mode fiber, DAQ: data acquisition card, TS: translation stage, Con.L: conical lens, L1: convex lens, L2 & L3: achromatic lens, RA: right-angle prism, RP: rhomboid prism, OC: optical condenser, M: mirror, SP: slip plate, LT: lens tube, TM: translation mount, KMM: kinematic mirror mount, and AL: acoustic lens. (**b**) Photograph of the prototype AR-OR-PAM system. (**c**) Close-up of the optoacoustic beam combiner. (**d**) Close-up of the optical condenser with a UST at the center. Reprinted from reference[34] with permission. Please click here to view a larger version of this figure.

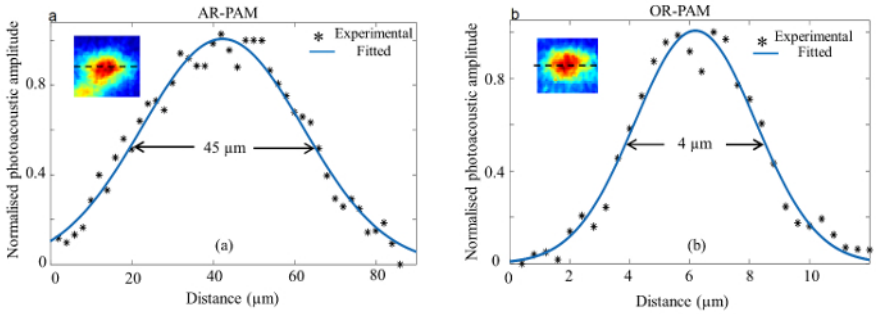

Figure 2: Lateral Resolution Test of the AR-OR-PAM System: Lateral resolution estimated by imaging gold nanoparticles ~100 nm in diameter. Black (*) dots: photoacoustic signal; blue line: Gaussian-fitted curve for (**a**) AR-PAM and (**b**) OR-PAM. The inset shows the representative AR-PAM image in (a) and OR-PAM image in (b) of the single gold nanoparticle. Reprinted from reference[34] with permission. Please click here to view a larger version of this figure.

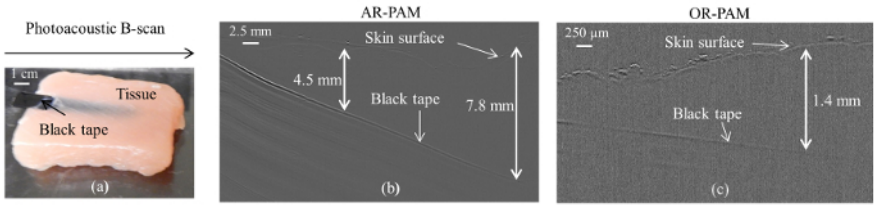

Figure 3: Imaging Depth Measurements: Single B-scan PA image of a black tape inserted obliquely onto chicken tissue. (**a**) Schematic diagram. (**b**) AR-PAM image. (**c**) OR-PAM image. Reprinted from reference[34] with permission. Please click here to view a larger version of this figure.

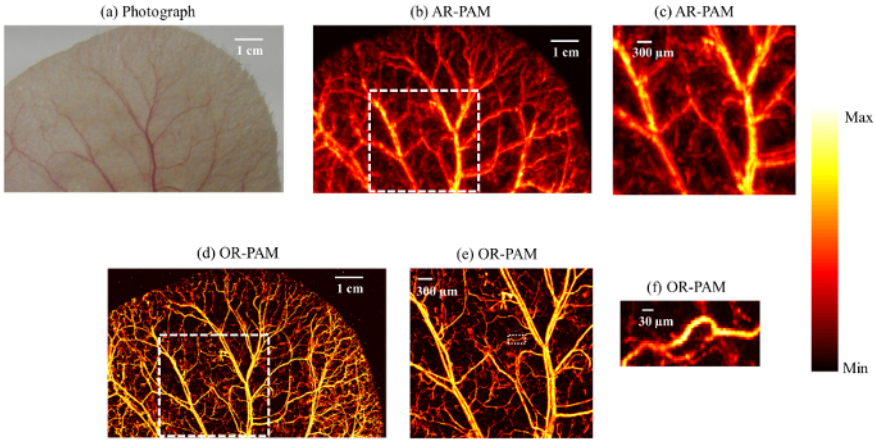

Figure 4: *In Vivo* Photoacoustic Image of a Mouse Ear: (**a**) Photograph of the mouse ear vasculature. (b) AR-PAM image. (**c**) Close-up of the region of interest (ROI) in (**b**), as shown by a white dashed line. (**d**) OR-PAM image. (**e**) Region of interest (ROI) in (**d**), as shown by a white dotted line. (**f**) Close-up image of the ROI white line in (e) showing a single capillary. Reprinted from reference[34] with permission. Please click here to view a larger version of this figure.

Discussion

In conclusion, a switchable AR and OR PAM system that can achieve both high-resolution imaging at lower imaging depths and lower-resolution imaging at higher imaging depths has been developed. The lateral resolution and imaging depth of the switchable system was determined. The advantages of this switchable PAM system include: (1) the high-resolution imaging using tight optical focusing; (2) the deep-tissue imaging using acoustic focusing; 3) the dark-field illumination for AR-PAM, which prevents strong PA signals from appearing on the skin surface; 4) the ability to keep the sample in one place, without moving it between different systems; 5) the possibility to avoid using multiple lasers and scanning stages; and 6) the minimal use of homemade components. This is the first reported combination of OR-PAM and dark-field AR-PAM that provides high-resolution, shallow-depth images and low-resolution, deep-tissue images of the same sample without moving the sample/object. The use of the same scanning stage and laser makes the system efficient as well as cost-effective. The combined system has a 4 µm lateral resolution with a 1.4 mm imaging depth, as well as a 45 µm lateral resolution with a 7.8 mm imaging depth. The system is made of an optical cage system with minimal homemade components, making it easier to assemble, align, and switch between the AR and OR PAM. The combined scanning head is compact and can easily be assembled on a single scanning stage. Using the combined system, *in vivo* imaging was successfully demonstrated.

The developed system can be used for pre-clinical imaging. Major preclinical applications include the imaging of angiogenesis, tumor microenvironments, microcirculation, drug response, brain functions, biomarkers, and gene activities. The limitations of the system include the scanning time. A long scanning time is currently needed, but it can be reduced by acquiring data in both directions. Simultaneous image acquisition between OR-PAM and AR-PAM is not possible at present. Currently, manual switching between OR-PAM and AR-PAM is necessary, which can be avoided by using a translation stage that has at least 10 cm Y-directional movement. Critical steps in the protocol include the confocal determination of the optical and acoustic focus; the achievement of an optical spot sizes less than 5 µm for OR-PAM, to image single capillaries; and the design of the optoacoustic beam combiner for the OR-PAM and of the optical condenser for the AR-PAM.

Disclosures

All animal experiments were performed according to the approved guidelines and regulations of the Institutional Animal Care and Use Committee of Nanyang Technological University, Singapore (Animal Protocol Number ARF-SBS/NIE-A0263). The authors have no relevant financial interests in the manuscript and no other potential conflicts of interest to disclose.

Acknowledgements

The authors would like to acknowledge the financial support from a Tier 2 grant funded by the Ministry of Education in Singapore (ARC2/15: M4020238). The authors would also like to thank Mr. Chow Wai Hoong Bobby for the machine shop help.

References

1. Hu, S., Wang, L. V. Photoacoustic imaging and characterization of the microvasculature. *J Biomed Opt.* **15** (1), 011101-01-011101-15 (2010).
2. Ntziachristos, V. Going deeper than microscopy: the optical imaging frontier in biology. *Nat Methods.* **7** (8), 603-614 (2010).
3. Wang, L. V., & Yao, J. A practical guide to photoacoustic tomography in the life sciences. *Nat Methods.* **13** (8), 627-638 (2016).
4. Zhou, Y., Yao, J., & Wang, L. V. Tutorial on photoacoustic tomography. *J Biomed Opt.* **21** (6), 061007 (2016).
5. Upputuri, P. K., Sivasubramanian, K., Mark, C. S. K., & Pramanik, M. Recent Developments in Vascular Imaging Techniques in Tissue Engineering and Regenerative Medicine. *BioMed Res Intl.* **2015** 9 (2015).
6. Yao, J., & Wang, L. V. Photoacoustic Brain Imaging: from Microscopic to Macroscopic Scales. *Neurophotonics.* **1** (1), 011003-1-011003-13 (2014).
7. Wang, L. V., & Hu, S. Photoacoustic Tomography: In Vivo Imaging from Organelles to Organs. *Science.* **335** (6075), 1458-1462 (2012).
8. Beard, P. Biomedical photoacoustic imaging. *Interface Focus.* **1** (4), 602-631 (2011).
9. Pan, D. *et al.* Molecular photoacoustic imaging of angiogenesis with integrin-targeted gold nanobeacons. *FASEB J.* **25** (3), 875-882 (2011).
10. Cai, X., Kim, C., Pramanik, M., & Wang, L. V. Photoacoustic tomography of foreign bodies in soft biological tissue. *J Biomed Opt.* **16** (4), 046017 (2011).
11. Pan, D. *et al.* Near infrared photoacoustic detection of sentinel lymph nodes with gold nanobeacons. *Biomaterials.* **31** (14), 4088-4093 (2010).
12. Wang, L. V. Multiscale photoacoustic microscopy and computed tomography. *Nat. Photon.* **3** (9), 503-509 (2009).
13. Zhang, E. Z., Laufer, J. G., Pedley, R. B., & Beard, P. C. In vivo high-resolution 3D photoacoustic imaging of superficial vascular anatomy. *Phys. Med. Biol.* **54** (4), 1035-1046 (2009).
14. Park, S., Lee, C., Kim, J., & Kim, C. Acoustic resolution photoacoustic microscopy. *Biomed.l Eng. Lett.* **4** (3), 213-222 (2014).
15. Zhang, H. F., Maslov, K., Stoica, G., & Wang, L. V. Functional photoacoustic microscopy for high-resolution and noninvasive in vivo imaging. *Nat. Biotechnol.* **24** (7), 848-851 (2006).
16. Maslov, K., Stoica, G., & Wang, L. V. In vivo dark-field reflection-mode photoacoustic microscopy. *Opt Lett.* **30** (6), 625-627 (2005).
17. Strohm, E. M., Moore, M. J., & Kolios, M. C. Single Cell Photoacoustic Microscopy: A Review. *IEEE J Sel Top Quantum Electron.* **22** (3), 6801215 (2016).
18. Kim, J. Y., Lee, C., Park, K., Lim, G., & Kim, C. Fast optical-resolution photoacoustic microscopy using a 2-axis water-proofing MEMS scanner. *Sci Rep.* **5,** 07932 (2015).
19. Matthews, T. P., Zhang, C., Yao, D. K., Maslov, K., & Wang, L. V. Label-free photoacoustic microscopy of peripheral nerves. *J Biomed Opt.* **19** (1), 016004, doi: 10.1117/1.JBO.19.1.016004(2014).
20. Hai, P., Yao, J., Maslov, K. I., Zhou, Y., & Wang, L. V. Near-infrared optical-resolution photoacoustic microscopy. *Opt Lett.* **39** (17), 5192-5195 (2014).
21. Danielli, A. *et al.* Label-free photoacoustic nanoscopy. *J Biomed Opt.* **19** (8), 086006 (2014).
22. Zhang, C. *et al.* Reflection-mode submicron-resolution in vivo photoacoustic microscopy. *J Biomed Opt.* **17** (2), 020501 (2012).
23. Hu, S., Maslov, K., & Wang, L. V. Second-generation optical-resolution photoacoustic microscopy with improved sensitivity and speed. *Opt Lett.* **36** (7), 1134-1136 (2011).
24. Konstantin Maslov, Hao F. Zhang, Song Hu & Wang, L. V. Optical-resolution photoacoustic microscopy for in vivo imaging of single capillaries. *Opt Lett.* **33** (9), 929-931 (2008).
25. Upputuri, P. K., Krishnan, M., & Pramanik, M. Microsphere enabled sub-diffraction limited optical resolution photoacoustic microscopy: a simulation study. *J Biomed Opt.* **22** (4), 045001 (2017).
26. Upputuri, P. K., Wen, Z.-B., Wu, Z., & Pramanik, M. Super-resolution photoacoustic microscopy using photonic nanojets: a simulation study. *J Biomed Opt.* **19** (11), 116003 (2014).
27. Allen, T. J. Novel fibre lasers as excitation sources for photoacoustic tomography and microscopy *et al.* in *Proc SPIE.* 97080W (2016).
28. Xing, W., Wang, L., Maslov, K., & Wang, L. V. Integrated optical-and acoustic-resolution photoacoustic microscopy based on an optical fiber bundle. *Opt Lett.* **38** (1), 52-54 (2013).
29. Estrada, H., Turner, J., Kneipp, M., & Razansky, D. Real-time optoacoustic brain microscopy with hybrid optical and acoustic resolution. *Laser Phys Lett.* **11** (4), 045601 (2014).
30. Jeon, S., Kim, J., & Kim, C. In vivo switchable optica- and acoustic - resolution photoacoustic microscopy. *Proc SPIE.* 970845 (2016).
31. Song, W. *et al.* Fully integrated reflection-mode photoacoustic, two-photon, and second Sci Rep. **6**,32240 (2016).
32. Park, J. *et al.*Delay-multiply-and-sum-based synthetic aperture focusing in Photoacoustic. *Biomed Opt.* **21** (3), 036010-10 (2016).
33. American National Standard for Safe Use of Lasers. *ANSI Standard Z136.*1-2000, NY. (2000).
34. Moothanchery, M., Pramanik, M., Performance Characterization of a Switchable Acoustic Resolution and Optical Resolution Photoacoustic Microscopy System. *Sensors.*, **17** (2), 357 (2017).

